Magnetic Flux Fluctuations Due to Eddy Currents and Thermal Noise in Metallic Disks

S. Uzunbajakau, A. P. Rijpma, J. Dolfsma, H. J. G. Krooshoop, H. J. M. ter Brake, M. J. Peters, and H. Rogalla, *Member, IEEE*

***Abstract*—We derive expressions for the magnetic flux in a circular loop due to eddy currents and thermal noise in coaxial metallic disks. The eddy currents are induced by an applied field that changes sinusoidally in time. We give expressions for the eddy current noise when the frequency of the applied field is very low as well as when it is very high. We combine these expressions to obtain one that is valid over the whole frequency range. The theoretical results agree well with experimental ones obtained by means of a superconducting quantum interference device (SQUID) magnetometer system. We also studied the flux due to thermal noise; again, the theoretical results show fair agreement with the experimental ones.**

***Index Terms*—Eddy currents, SQUID magnetometry, thermal noise.**

I. Introduction

VERY WEAK magnetic fields, such as biomagnetic fields, can be measured by means of superconducting quantum interference devices (SQUIDs), superconducting magnetometers cooled to cryogenic temperatures. Usually thermal shields are part of the cryostat, wires are shielded, and so are the SQUIDs. In other words, conducting objects are present during precise magnetic measurements. These objects give rise to disturbing fields due to thermal noise and eddy currents, the latter when subjected to a changing magnetic field. In this paper, analytical expressions for the disturbances due to the presence of a conducting circular disk will be deduced. These expressions will be evaluated by measurements. The expressions can be easily extended to cylindrical-shaped objects, so that they can be used to calculate the noise from an actual electromagnetic shield or thermal radiation shield that is composed of a hollow cylinder and a disk-shaped bottom.

A time-varying magnetic field gives rise to time-varying induced currents in conducting objects, and these currents in turn generate an additional field that tends to cancel the original field (Lentz's law). At high frequencies, a very thin layer carries most of the currents: this is called the skin effect. As a consequence, the magnetic field in the material decreases exponentially. At the so-called skin depth, the magnitude of the magnetic field is a factor 1/e times the surface value. We will restrict ourselves to disks with a homogeneous isotropic conductivity that are subjected to a homogeneous magnetic field that is changing sinusoidally in time. The magnetic permeability of the disks is that of free space (μ_0). Capacitive effects can be neglected. Consequently, in the very-low-frequency range, the attenuation of the magnetic field in the disk can be neglected. Contrarily, in the high-frequency limit, the field will not penetrate at all; the currents and the magnetic field will be confined to the surface of the disks. Expressions for the magnetic flux in a circular loop due to the eddy currents in the presence of various disks will be derived in both limiting cases (i.e., for very low and very high frequencies). The theoretical results will be checked by means of experiments. Empirically, it is found that in the frequency range between the two limits the disks act as high-pass filters. As a consequence, this enabled us to obtain an expression for the magnetic flux due to eddy currents that is valid in the entire frequency range that describes the experiments well.

Thermal noise is present in all objects that are electrically conducting. Each volume element generates a short-circuit noise current that generates, in turn, a fluctuating magnetic flux. The average value of the current in a volume element is zero. The root-mean-square value (time-averaged power) of these noise sources is defined by Nyquist's theorem. The frequency distribution of thermal noise power is uniform (i.e., white noise). Expressions for magnetic field fluctuations arising from thermal motion in an infinite conducting slab have been derived by Varpula and Poutanen [1]. Kasai *et al.* extended these calculations and obtained the magnetic field fluctuations at the axis of disks of finite extent [2]. In the present paper, expressions will be derived for the magnetic flux noise in a circular loop due to thermal noise in metallic disks. The theoretical results will be compared with experimental ones.

All measurements are carried out by means of a SQUID magnetometer system with a single circular coil acting as the sensor coil. The coil is parallel and coaxial with the conducting disk. The system is operated within a magnetically shielded room. The applied field used to induce the eddy currents is obtained from a set of Helmholtz coils.

II. Theory

A. Eddy Currents

First, we will consider eddy currents in a circular disk with radius r_{disk} and height h when a uniform field is applied perpendicular to the disk as depicted in Fig. 1.

1) Low-Frequency-Limited Case: Assumptions made are as follows.

a) The electric conductivity of the disk is homogeneous and isotropic.
b) The permeability everywhere (i.e., both in the conductor and outside the conductor) is that of free space (i.e., μ_0).

Manuscript received September 24, 2002; revised March 10, 2003.

The authors are with the Faculty of Applied Physics, University of Twente, 7500 AE Enschede, The Netherlands (e-mail: s.uzunbajakau@tn.utwente.nl).

Digital Object Identifier 10.1109/TMAG.2003.812720

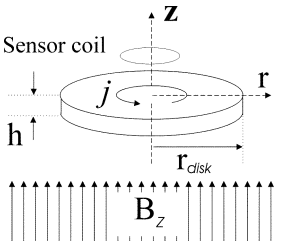

Fig. 1. Arrangement of the circular conducting disk and the sensor coil in an applied uniform magnetic field.

c) The disks used have a permittivity of free space and a conductivity higher than 10^6 S/m; hence, $\omega\varepsilon/\sigma \ll 1$ and as a consequence capacitive effects can be neglected for frequencies up to 1000 Hz, the highest frequency we consider [3].

In this section, we presume that the frequency of the applied field is very low, so that the skin depth $\delta = 1/\sqrt{\pi f \mu \sigma}$ is much larger than the height of the disk. The circular disk in the $z = 0$ plane has a specific resistance ρ. A changing uniform field is applied in the z direction. We consider concentric rings with radius r and width dr. From

$$\oint \vec{E} \cdot d\vec{l} = -\frac{d\Phi}{dt} \text{ and } \vec{j} = \sigma \vec{E} = \frac{\vec{E}}{\rho} \tag{1}$$

where j is the current density and σ the conductivity, it follows

$$2\pi r \rho j = -\pi r^2 \frac{\mathrm{dB}_z}{dt} \text{ or } j = -\frac{r}{2\rho}\frac{\mathrm{dB}_z}{dt}. \tag{2}$$

The ring-shaped segments of the disk form coplanar circuits. Consequently, the flux in the sensor coil of the magnetometer due to the eddy currents is

$$\Phi_{\omega\downarrow 0} = \int_0^{r_{\mathrm{disk}}} M(r) j(r) h dr \tag{3}$$

where $M(r)$, the mutual inductance between a ring-shaped segment of the disk and the coil, is given in the Appendix [(A2), inserting for r_1 the radius of the sensor coil, for z the distance between disk and sensor coil and $r_2 = r$].

2) High-Frequency-Limited Case: At very high frequencies, the currents and magnetic field are confined to the surface of the disk. As the magnetic field cannot penetrate the disk, the normal component of the magnetic field must vanish on its surface. The magnetic field around a thin disk can be calculated by solving the Laplace equation and applying the proper boundary equations. For a thin disk, the problem has been solved by Overweg and Walter-Peters [4] for the flux in a sensor coil with radius r_{sensor} that is parallel and coaxial to the disk

$$\Phi_{\omega\uparrow\infty} = 2r_{\mathrm{sensor}}^2 B_{\mathrm{appl}} \left(\frac{\nu}{\nu^2+1} - \operatorname{arc\,cot}(\nu) \right) \tag{4}$$

where

$$\nu^2 = \frac{1}{2r_{\mathrm{disk}}^2} \left(z^2 + r_{\mathrm{sensor}}^2 - r_{\mathrm{disk}}^2 + \left[\left(z^2 + r_{\mathrm{sensor}}^2 - r_{\mathrm{disk}}^2 \right)^2 + 4r_{\mathrm{disk}}^2 z^2 \right]^{1/2} \right) \tag{5}$$

where z is the distance between disk and sensor coil.

3) Frequency Range Between the Low- and High-Frequency-Limited Case: We presume that the relation between the applied flux and the flux in the sensor coil due to eddy currents can adequately be described by

$$\frac{\Phi_{\mathrm{eddy}}}{\Phi_{\mathrm{appl}}} = c \times \frac{-i\frac{\omega}{\omega_0}}{1 + i\frac{\omega}{\omega_0}}. \tag{6}$$

In the high-frequency limit, this expression reads

$$\lim_{\omega\to\infty} \frac{\Phi_{\mathrm{eddy}}}{\Phi_{\mathrm{appl}}} = \frac{\Phi_{\omega\uparrow\infty}}{\Phi_{\mathrm{appl}}} = -c \tag{7}$$

and in the low-frequency limit

$$\lim_{\omega\to 0} \frac{\Phi_{\mathrm{eddy}}}{\Phi_{\mathrm{appl}}} = \frac{\Phi_{\omega\downarrow 0}}{\Phi_{\mathrm{appl}}} = -i\frac{\omega}{\omega_0} c. \tag{8}$$

Thus, the constant c can be calculated using (4) and (5) and, subsequently, the constant ω_0 can be calculated using (3).

B. Thermal Noise

The disk depicted in Fig. 1 can be viewed as a collection of infinitesimal volume elements. Each volume element generates a noise current dipole [1]. Each current dipole (and its accompanying volume current) creates a magnetic field. The current dipoles are not correlated, so at any location the resulting magnetic field noise from the whole disk is obtained by summing the power of the field noise resulting from the separate elements. As the elements are continuously distributed they can be integrated. The contribution to the magnetic field in the z direction caused by current dipoles in the radial direction is zero. The contribution of current dipoles in the z direction is also zero. So the only contributing elements are the current dipoles that have a tangential direction. These current dipoles are the primary sources. However, a magnetic field is the superposition of the fields due to primary sources and volume currents. The volume currents can be described by means of imaginary sources, so-called secondary sources [5]. The secondary sources are current elements that are perpendicular to interfaces between regions of different conductivity. Consequently, the secondary sources in the circular disk displayed in Fig. 1 will be in the z direction and in the radial direction. Hence, the volume elements do not contribute to the z component of the magnetic field on the axis. So the only contributing elements to the z component of the magnetic field on the axis are the tangential components of the primary sources. Next, a subset of the "infinitesimal" volume elements is considered. This subset is chosen such that its elements establish a ring-shaped segment with radius r, width dr, and height dh. It is assumed that their combined contribution to the noise field can be obtained by considering the ring as a resistance and calculating the short-circuited electrical current noise according to Nyquist's theorem

$$\overline{i_{\mathrm{ring}}^2} = \frac{4k_B T \Delta f}{\Delta R} \tag{9}$$

where k_B is the constant of Boltzmann and ΔR the resistance of the ring, that reads

$$\Delta R = \frac{2\pi r}{\sigma dr dh} \tag{10}$$

leading to

$$\overline{i_{\mathrm{ring}}^2} = 4k_B T \sigma \Delta f \frac{dr dh}{2\pi r}. \tag{11}$$

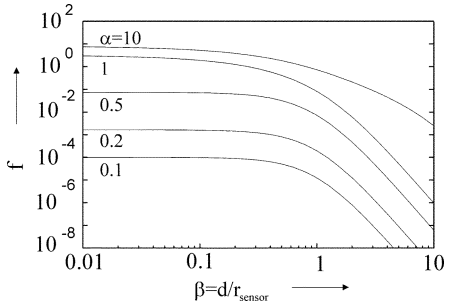

Fig. 2. Function f describing the thermal noise of a thin conducting disk for various values of $\alpha = r_{\rm disk}/r_{\rm sensor}$ as a function of $\beta = d/r_{\rm sensor}$.

TABLE I
PARAMETERS DESCRIBING THE METALLIC DISKS USED IN THE EXPERIMENTS

Material	Conductivity (S/m)	Skin depth at 1000Hz (mm)	Thickness (mm)	Diameter (mm)
Copper	5.37×10^7	2.2	0.10	83
Copper	4.44×10^7	2.4	0.50	83
Copper	4.79×10^7	2.3	1.00	83
Copper	4.62×10^7	2.3	3.00	83
Copper	4.44×10^7	2.4	0.50	40
Lead	0.445×10^7	7.5	0.50	83
Brass	1.45×10^7	4.2	0.50	83
Steel	0.143×10^7	13	0.50	83

The mean square value of the flux through a coil parallel to the disk, assuming that the disk is thin (i.e., $h \ll d$, where d is the distance between disk and sensor coil), is

$$\overline{\Phi^2} = \frac{4k_B T\sigma h\Delta f}{2}\int_0^{r_{\rm disk}} M^2(r)\frac{dr}{r} \tag{12}$$

where M is given in the Appendix [(A2) with $r_1 = r$, $r_2 = r_{\rm sensor}$, and $z = d$]. Expression (12) can be solved numerically for any disk and sensor coil that are coaxial.

In order to obtain a result that can be used without the need to solve (12), the function f is introduced

$$f(\alpha,\beta) = \frac{8}{\pi}\left(\frac{2}{\mu_0}\right)^2\int_0^1 \frac{M^2(\alpha\rho,\beta)}{2\pi\rho}d\rho \tag{13}$$

where $\alpha = r_{\rm disk}/r_{\rm sensor}$ and $\beta = d/r_{\rm sensor}$.

Whenever the values of $r_{\rm disk}$, $r_{\rm sensor}$, and d are known, the flux noise can be obtained from the plot given in Fig. 2 by the following:

$$\overline{\Phi^2} = \pi\cdot r_{\rm sensor}^2\cdot\left(\frac{\mu_0}{2}\right)^2\frac{k_B T}{2}\cdot\sigma\cdot h\cdot f(\alpha,\beta). \tag{14}$$

III. METHOD

Measurements were carried out on eight disks that varied in conductivity or dimensions. Their parameters are given in Table I. All disks were cut from metal sheets. Strips were made from the same sheets to measure the conductivity by means of the four-point method.

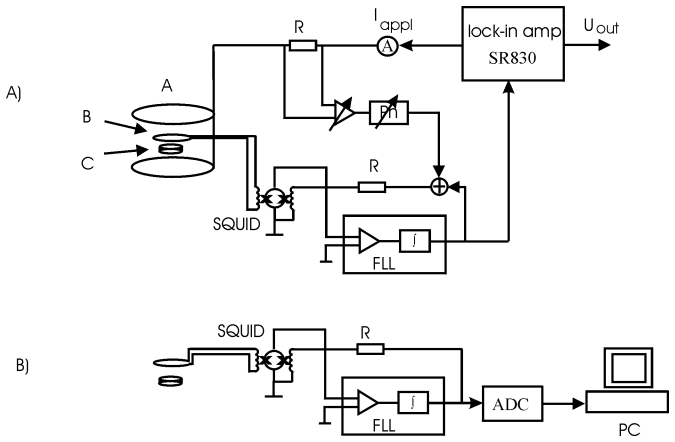

Fig. 3. (a) Experimental setup for the measurement of the flux due to eddy currents in a conducting disk. The Helmholtz coil is indicated by A, the sensor coil by B, the disk by C, and the adjustable phase shifter by Ph. (b) Experimental setup for the measurement of the flux due to thermal noise in a conducting disk.

A. Eddy Currents

The influence of eddy currents was measured as the ratio of the flux in a sensor coil due to eddy currents and the flux due to the applied field. The experimental setup is sketched in Fig. 3(a). A low-T_c SQUID was used as a sensor. The SQUID is a magnetic flux-to-voltage converter with a nonlinear input-output characteristic. In order to linearize this characteristic, the SQUID was operated as a zero-detector in a flux-locked loop [FLL in Fig. 3(a)]. A more detailed description of the SQUID and FLL that were used can be found in [6], [7]. The effective area of a bare SQUID is relatively small yielding a relatively low sensitivity to the magnetic field. In order to increase the sensitivity, a superconductive flux transformer was used consisting of a sensing coil and an input coil that was inductively coupled to the SQUID. The intrinsic noise of the measurement setup was white in the frequency region above 1 Hz. The level of the white noise was 5 fT/$\sqrt{\rm Hz}$. The bandwidth of the measurement setup (SQUID plus FLL) was 2 kHz. The sensor coil with a diameter of 30 mm was positioned at a point midway between a set of Helmholtz coils. In order to measure the flux due to eddy currents as accurately as possible, a compensation circuit was used consisting of an adjustable amplifier and an adjustable phase shifter. For each frequency, the measurements were performed in two steps.

During the first step, a magnetic field was applied without any disk present. By simultaneous adjustment of the amplifier and phase shifter, the signal due to the applied field was compensated (balanced), nullifying as much as possible the output voltage of the flux-locked loop (FLL). The applied current $I_{\rm appl}$ and the remaining output voltage $U_{\rm out}$ were recorded defining the initial imbalance. This was done to verify that the amplitude of $U_{\rm out}$ due to the initial imbalance is well below that due to eddy currents. The output voltage of the SR830 lock-in amplifier $U_{\rm out}$ is a complex quantity. Its magnitude is equal to the output voltage of the FLL and its phase is equal to the phase difference between the applied current $I_{\rm appl}$ and the output voltage of the FLL. During the second step, a disk was placed in the appropriate position underneath the cryostat and the output voltage $U_{\rm out}$ was recorded again. As the flux applied by the Helmholtz coils was compensated in the first step of the measurement, the

output voltage is proportional to the flux due to eddy currents. From Fig. 3(a), one can deduce an expression for the influence of eddy currents in terms of imbalance as

$$\frac{\Phi_{\text{eddy}}}{\Phi_{\text{appl}}} = \frac{\frac{U_{\text{out}}}{H_2(i\omega)}}{I_{\text{appl}} \cdot H_1(i\omega)} = \frac{U_{\text{out}}}{I_{\text{appl}}} \frac{1}{H_1(i\omega) \cdot H_2(i\omega)} = \frac{U_{\text{out}}}{I_{\text{appl}}} \frac{1}{H(i\omega)} \quad (15)$$

where Φ_{eddy} is the flux in the sensor coil due to eddy currents and $\Phi_{\text{appl}} = B_{\text{appl}} \times \pi r_{\text{sensor}}^2$. The transfer function $H(i\omega)$, which relates the applied current and the output voltage, was measured separately (compensation circuit was open).

For six disks, the ratio in magnitudes and difference in phase between the eddy current flux and the applied flux were measured as a function of the frequency of the applied field and as a function of the distance between disk and sensor coil of the magnetometer. Theoretical values of the ratio of the amplitudes of Φ_{eddy} and Φ_{appl} were calculated using (3) and (6).

B. Thermal Noise

The thermal noise measurements were carried out in the bandwidth from 1 Hz to 1 kHz. The measurement setup is depicted in Fig. 3(b). The thermal noise was recorded of eight disks and a power spectral density was calculated using Welch's method and a Hanning window. Subsequently, the white noise levels were estimated from the power spectra density by averaging the spectra in frequency regions where no other spectral components ($1/f$ noise at low frequencies, noise due to vibrations, power line interference and its harmonics) were present. From the resultant white noise levels, the intrinsic noise of the measurement system was subtracted. The level of the intrinsic system white noise was measured without any conducting disk present.

The flux due to thermal noise was measured as a function of the distance between the disk and the sensor coil, the thickness of the disk, and the conductivity of the disk. Two different sensor coils were used of 30- and 50-mm diameter, respectively. The thermal flux noise was calculated for all eight disks using (12). The results are expressed in terms of field noise, i.e., the measured flux divided by the area of the sensor coil.

As mentioned previously, the flux noise generated by a disk is only due to the presence of primary sources. However, if the disk is cut into pie-shaped pieces that are electrically insulated from each other, secondary sources are present at the sides of the wedges. These secondary sources are tangentially orientated. Consequently, these secondary sources will contribute to the magnetic field in the z direction. This contribution counteracts the contribution of the primary sources. Hence, the combination of the pie-shaped pieces should generate a lower level of field noise in the sensor coil than the original intact disk. However, if the disk is cut so that it forms a smaller disk and a concentric ring, the secondary sources at the interface have a radial orientation and, hence, they will not contribute to the magnetic flux in the sensor coil. In order to validate these assumptions, two copper disks with a thickness of 0.5 mm and diameter 83 mm were cut in pieces. One was cut so that it formed a disk with a diameter of 40 mm that fitted in a ring with an inner diameter of 40 mm and an outer diameter of 83 mm. The two pieces were insulated from each other during measurements. The second disk was divided in pieces shaped like wedges of pie. The number of wedges was varied from 2 to 16. All wedges were electrically insulated from each other.

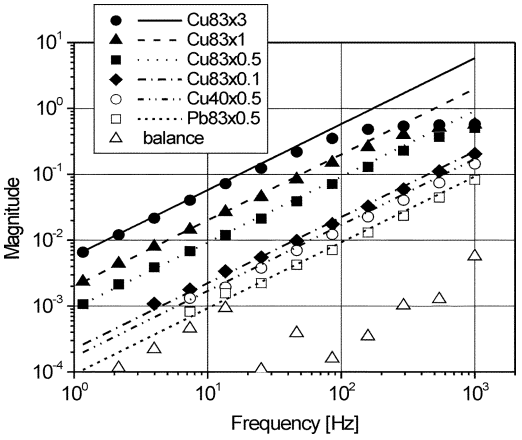

Fig. 4. Ratio of the amplitude of the eddy current flux and that of the applied flux as a function of the frequency for the various disks. The lines represent the theoretical values in the low-frequency limit calculated using (3). The markers indicate the measurements. The open triangles depict the balance of the applied flux, i.e., the residual signal after compensation of the applied flux. The balance defines the minimum value that can be measured using the experimental setup.

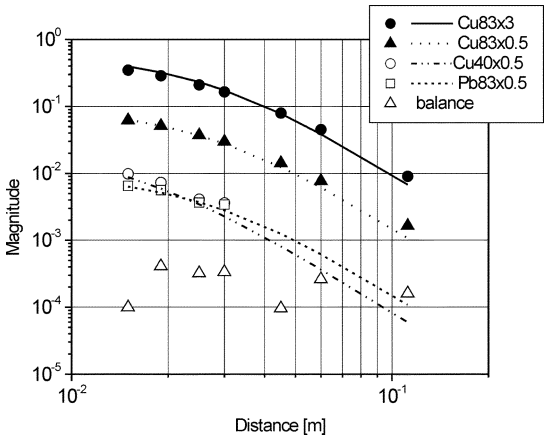

Fig. 5. Ratio of the amplitude of the eddy current flux and that of the applied flux as a function of the distance between the disk and the sensor coil. The frequency of the applied field was 85 Hz, where the low-frequency approximation given by (3) is valid. The lines represent the theoretical values, the markers the measured ones. The open triangles depict the balance of the applied flux, i.e., the residual signal after compensation of the applied flux. The balance defines the minimum value that can be measured using the experimental setup.

IV. Results

A. Eddy Currents

Typical results for the flux due to eddy currents are shown in Figs. 4–6. In Fig. 4 the magnetic flux in the sensor coil divided by the applied flux is shown as a function of the frequency. The lines represent theoretical values derived for the low-frequency-limited case, and the markers are the measured values. Fig. 5 shows the flux in the sensor coil as a function of the distance. The lines correspond to the theoretical values derived for the low-frequency-limited case.

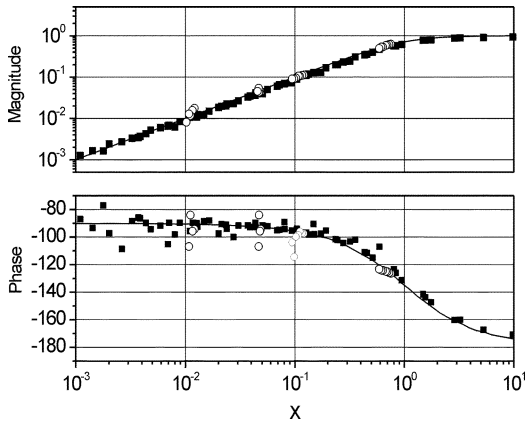

Fig. 6. Amplitude and phase of $G(x)$ [see (16)] describing the relationship between the flux in the sensor due to eddy currents and the flux due to the applied magnetic field. The solid curves represent amplitude and phase of $G(x)$. Experimental data presented in Figs. 4 and 5 are described by black squares and open circles, respectively.

To emphasize the validity of (6), the measured and theoretical data that are presented in Figs. 4 and 5 are depicted in a single graph in the following way. Rearranging the terms in (6) yields

$$G(x) = \frac{\Phi_{\text{eddy}}}{\Phi_{\text{appl}}}\frac{1}{c} = -\frac{i\frac{\omega}{\omega_0}}{1+i\frac{\omega}{\omega_o}} = -\frac{ix}{1+ix}. \qquad (16)$$

The function $G(x)$ does not depend on parameters describing the disks or the applied field. For this reason, all experimental data presented in Figs. 4 and 5 are expected to collapse into two curves (amplitude and phase) described by $G(x)$. Both the theoretical and experimental values obtained for the magnitude and the phase of $G(x)$ are shown in Fig. 6.

B. Thermal Noise

The results of the thermal noise flux measurements are shown in Figs. 7–10. Again, the line shows the theoretical value and the markers the measured ones. The intrinsic system noise of 25 fT^2/Hz is subtracted from the measured values. The results show a fair agreement between theoretical and experimental results.

Commonly, the mean square value of the flux in the sensor coil is approximated by

$$\overline{\Phi^2} = \overline{B_{z,\text{disk}}^2} \times \pi r_{\text{sensor}}^2 \qquad (17)$$

using an expression for $\overline{B_{z,\text{disk}}^2}$ that is derived by Kasai *et al.* [2]. The dotted lines in Fig. 9 show this approximation. Measurements of thermal noise versus distance were performed using two types of sensor coils with diameters of 30 and 50 mm. In Fig. 9, the results are shown for the sensor coil of 50 mm. Comparison of the results obtained with the two sensor coils shows that (3) approximates the experimental data better than (17). This is especially true in practical cases where the distance between the sensor coil and the conducting disk is small and the diameter of the sensor coil is about the same as that of the conducting disk.

The flux noise level resulting from the two concentric parts cut from one disk was 95 $\text{fT}/\sqrt{\text{Hz}}$ and 117 $\text{fT}/\sqrt{\text{Hz}}$ for the disk-shaped part and the ring, respectively. When the two pieces were combined to one disk but keeping the two pieces insulated

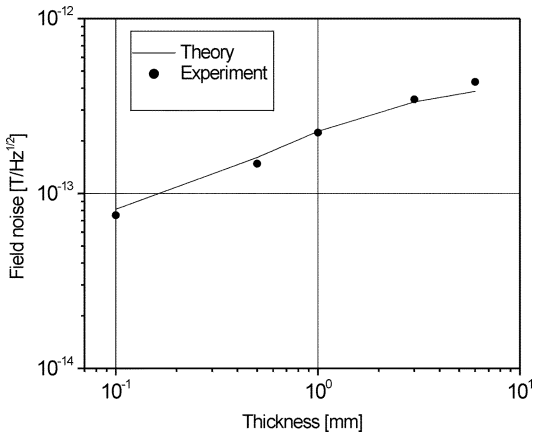

Fig. 7. Thermal flux noise in copper disks as a function of the thickness of the disks. The diameter of the sensor coil was 30 mm and the distance between disks and sensor coil was 10 mm.

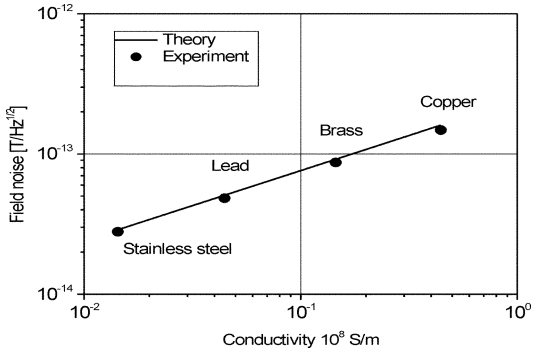

Fig. 8. Thermal flux noise due to disks of 83-mm diameter and 0.5-mm thickness as a function of conductivity. The diameter of the sensor coil was 30 mm and the distance between disks and sensor coil was 10 mm.

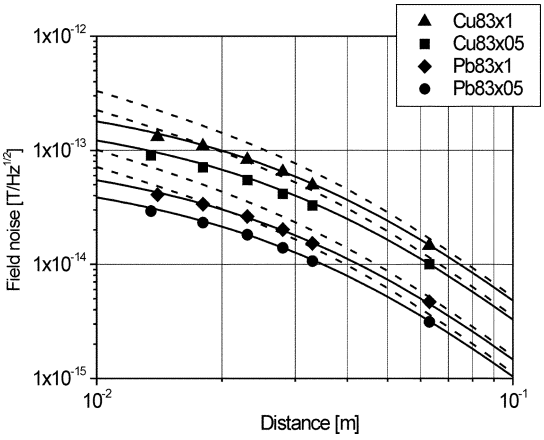

Fig. 9. Thermal flux noise as a function of the distance between the disks and a sensor coil with a diameter of 50 mm. The intrinsic SQUID noise was subtracted from the measurements. The solid lines indicate the theoretical values given by (12). The dashed lines show the approximation $(\overline{B_z^2}\pi r_{\text{sensor}}^2)^{1/2}$. Pb 83×1 stands for two disks Pb 83×0.5 placed one on top of the other.

from each other, a noise level of 146 $\text{fT}/\sqrt{\text{Hz}}$ was recorded, whereas the noise level from the original disk was 151 $\text{fT}/\sqrt{\text{Hz}}$. So, the noise level from the two combined parts is equal to $\sqrt{95^2+117^2} \approx 151$ $\text{fT}/\sqrt{\text{Hz}}$ being the same as that from the original disk. This is in accordance with expectation, because the secondary sources have a radial direction on the interface. The primary sources are the same for the combination of the

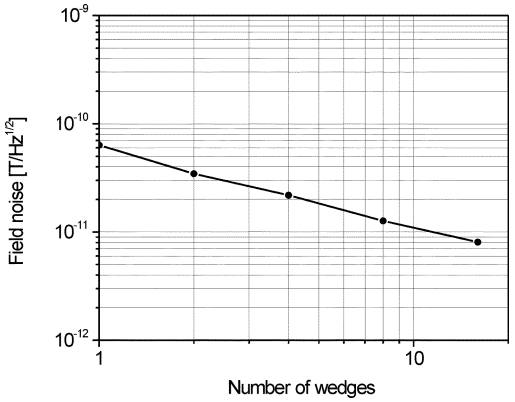

Fig. 10. Thermal flux noise as a function of the number of wedges in a circular disk at a distance of 10 mm from a sensor coil with a diameter of 30 mm.

two pieces and the original disk. This validates assumptions that were made in deriving (12). However, due to the presence of the tangential secondary sources at the interface, the flux noise of the disk cut in wedge-shaped pieces is decreased when the noise level from the combined pieces are compared with that from the original intact disk. The noise level decreases with the number of wedges as shown in Fig. 10, as the number of interfaces increases.

V. Discussion

Theoretical values for the flux due to eddy currents were derived for low frequency and high frequencies. Empirically an expression was found for the entire frequency range. Measured and theoretical values are in agreement for different parameters, i.e., the conductivity, diameter and thickness of the disk, the separation between the disk and sensor coil, and the frequency of the applied magnetic field. Consequently, the conclusion that (6) describes the flux in the entire frequency range seems to be justified.

Also, the correspondence between theory and experiment for thermal noise is good. The correspondence is much better using (3) than using (17). Cutting the disk in wedge-shaped pieces helps to reduce the thermal noise. In this case, the volume currents contribute to the thermal flux noise as the secondary sources are in the tangential direction. The volume currents always counteract the magnetic field generated by the primary sources; hence, the thermal flux noise is reduced. Cutting the disk in a disk plus ring will not affect the thermal noise because the primary and secondary sources present in the original disk will not change.

It is easy to extend the theory to cylindrical objects that are coaxial with the sensor coil [8] enabling the calculation of the noise generated in an actual thermal shield.

Appendix

Mutual Inductance Between Two Coaxial Circular Current Loops

The mutual inductance between two coaxial circular loops with radii r_1 and r_2 that are in two planes separated by a distance z is [9]

$$\begin{aligned} M &= \frac{\mu_0}{4\pi}\oint\oint \frac{d\vec{s}\cdot d\vec{s}'}{R} = \frac{\mu_0 r_1 r_2}{4\pi} \\ &\quad \times \int_0^{2\pi}\int_0^{2\pi} \frac{\cos(\theta-\theta)' d\theta d\theta'}{(r_1^2+r_2^2+z^2-2r_1r_2\cos(\theta-\theta'))^{1/2}} \\ &= \mu_0 r_1 r_2 \int_0^{\pi} \frac{\cos\Psi d\Psi}{(r_1^2+r_2^2+z^2-2r_1r_2\cos\Psi)^{1/2}} \end{aligned}$$

where $\Psi = \theta - \theta'$ (A1)

leading to

$$M = \frac{2\mu_0\sqrt{r_1 r_2}}{k}\left[\left(1-\frac{k^2}{2}\right)K(k) - E(k)\right] \tag{A2}$$

with

$$k^2 = \frac{4r_1r_2}{z^2+(r_1+r_2)^2}. \tag{A3}$$

$K(k)$ and $E(k)$ are complete elliptic integrals of the first and second kind and are given by

$$K(k) = \int_0^{\pi/2} \frac{d\alpha}{\sqrt{1-k^2\sin^2\alpha}} \tag{A4}$$

$$E(k) = \int_0^{\pi/2} \sqrt{1-k^2\sin^2\alpha}\, d\alpha. \tag{A5}$$

References

[1] T. Varpula and T. Poutanen, "Magnetic field fluctuations arising from thermal motion of electric charge in conductors," *J. Appl. Phys.*, vol. 55, pp. 4015–4021, 1984.

[2] N. Kasai, K. Sasaki, S. Kiryu, and Y. Susuki, "Thermal magnetic noise of dewars for biomagnetic measurements," *Cryogenics*, vol. 33, pp. 175–179, 1993.

[3] R. Plonsey and D. B. Heppner, "Considerations of quasistationarity in electrophysiological systems," *Bull. Math. Biophys.*, vol. 29, pp. 657–664, 1967.

[4] J. A. Overweg and M. J. Walter-Peters, "The design of a system of adjustable superconducting plates for balancing a gradiometer," *Cryogenics*, pp. 529–534, 1987.

[5] J. Sarvas, "Basic mathematical and electromagnetic concepts of the biomagnetic inverse problem," *Phys. Med. Biol.*, vol. 32, pp. 11–22, 1987.

[6] H. J. M. ter Brake, J. Flokstra, W. Jasszczuk, R. Stammis, G. K. van Ancum, A. Martinez, and H. Rogalla, "The UT 19-channel DC SQUID based neuromagnetometer," *Clin. Phys. Physiol. Meas.*, vol. 12, pp. 45–50, 1991.

[7] J. Flokstra, D. J. Adelerhof, E. P. Houwman, D. Veldhuis, and H. Rogalla, "Josephson junctions and DC SQUIDS based on Nb/Al technology," *Clin. Phys. Physiol. Meas.*, vol. 12, pp. 59–66, 1991.

[8] A. P. Rijpma, "Fetal heart monitor," Ph.D. dissertation, Univ. Twente, Enschede, The Netherlands, 2002.

[9] P. C. Clemmow, *An Introduction to Electromagnetic Theory*. Cambridge, U.K.: Cambridge Univ. Press, 1973, pp. 143–145.